

# Deturbidization of vegetable oil refinery wastewater with extracted fish scale biomass via coagulation process; Non-linear kinetics studies

## Abstract

Chito-protein was successfully synthesized from fish scale. The ability of a coagulant (chito-protein) prepared from fish scale (FSC) to carry out an effective removal of pollutants from food processing industry (vegetable oil industry wastewater, VOW) was evaluated at bench scale using a simulated jar test analysis. The coagulant was characterized via proximate analysis and instrumental analysis: Fourier transform infrared spectroscopy (FTIR) and scanning electron microscopy (SEM). The maximum kinetic parameters determined were recorded at  $K$  of  $2 \times 10^{-5} \text{L/mg.min}$ ,  $1 \text{g}$ ,  $t_{1/2} = 50 \text{ min}$ ,  $R^2 = 0.9245$  and  $\text{pH}$  of 2. Regression coefficient analysis ( $R^2$ ) was used to ascertain the accuracy of the fit to the postulated kinetic model. However, it was concluded that the second order kinetic model described the reaction most adequately. Removal efficiency of turbidity (87.21%) was obtained at optimum contact time of 30 min,  $\text{pH}$  2, coagulant dosage of 1.5g and temperature of 323K. Kinetic study showed that Pseudo first order and pseudo second order models were the best two models in describing the coag-adsorptive kinetics of the coagulant. Similarly, the predicted kinetic data were adjudged statistically significant using F- test and T-test.

**Keywords: Wastewater, coagulation, fish scale, turbidity, kinetic model, non-linear**

## 1.0 INTRODUCTION

Rapid industrialization has led to generation and unwholesome disposal of contaminated wastewater. Food processing (abattoir, vegetable oil etc.), paint, textile, pharmaceutical, cosmetics and plastic industries are among the industries that generates large volume of wastewater. Most of these wastewaters contain toxic substances (Okey-Onyesolu et al. (2016), high organic and inorganic dissolved solids, COD, BOD, and oil end which can be harmful if discharged untreated. The treatment of vegetable oil refinery wastewater (VOW) has been a major issue of environmental concern. Refining of crude vegetable oils generates large amounts of wastewater, which come from the degumming, de-acidification, deodorization and neutralization steps (Dkhissi et al., 2018). Its characteristics depend largely

37 on the type of oil processed, resulting in both high inorganic as well as organic pollutants  
38 Moka (2015). Many processing techniques have been employed in the fight against pollution  
39 in VOW, a wide variety of physicochemical processes has been proposed  
40 (coagulation/flocculation, adsorption, photocatalysis, electrocoagulation, membrane  
41 filtration) [Dkhissi et al., 2018]. Oil refinery wastewater treatment have gained increasing  
42 importance, it can be treated either separately or in conjunction by chemical or biological  
43 means. Biological treatment methods offer an easy and cost effective alternative to chemical  
44 methods. Coagulation and flocculation as a unit process, in water and wastewater treatment  
45 entails the use of metal salts (Al and Fe salts) (Xu et al, 2009). Also, the coagulation process  
46 is one of the most effective methods of reducing/removing pollutants from wastewater. But  
47 there are problems associated with chemical treatment which includes; the increased handling  
48 costs and the production of chemical sludge that is difficult to treat (Dkhissi et al., 2018).  
49 However, studies have discovered a number of drawbacks concerning the use of these  
50 conventional coagulants. For example, Alzheimer's disease and other related problems are  
51 associated with residual alum in treated water (Divakaran et al, 2001). To solve this problem  
52 many types of natural reagents have been developed for removing pollutants from wastewater  
53 chitosan (Roussy et al, 2005), tannins (Ozacar et al, 2002), aqueous extract of the seed of  
54 moringa oleifera; extract of plantain peelings ash (Oladoja, 2008); and extracts of okra and  
55 nirmali seed (Ani et al, 2010), they have advantages of being biodegradable and without risk  
56 to public health, so a number of plant, animal or micro- organism sources are used in  
57 wastewater treatment.

58 The present paper aims to valorise the fish scale chito-protein as a techno – economically and  
59 eco-friendly coagulant for the treatment process of wastewater taken from vegetable oil  
60 refining industry located at the south-east of Nigeria. The effects of the main experimental  
61 conditions (initial solution pH, coagulant dosage, settling time and operating temperature) on  
62 the coagulation treatment performance were studied. The coagulation process performance in  
63 all cases was evaluated by means of the turbidity (TDSP).

64

## 65 **2.0 MATERIALS AND METHODS**

### 66 **2.1 Effluent collection and analysis**

67 A sample of vegetable oil refinery wastewater (VOW) was collected from an oil refinery  
68 industry located in Onitsha, Anambra State, Nigeria and stored at room temperature. The  
69 vegetable oil refinery effluent was preserved in dark plastic container to avoid photo-

70 reactions. The vegetable oil refinery wastewater sample was characterized before and after  
71 treatment using standard methods (APHA, 1998).

72

### 73 **2.2 Processing of the coagulant from fish scale (FS)**

74 The fish scale (FS) was obtained from Otuocha market in Anambra East, Anambra state of  
75 Nigeria. The FS (Fig. 1) was washed thoroughly with water to remove unwanted materials  
76 and sun dried for 14 days. It was crushed using a pestle and mortar to reduce the size. The  
77 crushed sample was further air dried for five days to remove possible remaining moisture.  
78 The FS sample was then transformed into powder using a grinding machine and sieved with a  
79 laboratory sieve of known mesh size.

80 The powdered FS (Figure 2) was then processed into a coagulant (FSC), by adopting  
81 modified Fernandez-Kim method described by (Ani et al., 2011). The product of  
82 deproteinization of fish scale flour (FSF) was utilized instead of chitosan. For the  
83 deprotenization, 1 L of 1M NaOH solution containing 100 g of FSF was stirred continuously  
84 at 70 °C for 2h. The mixture was allowed to settle and cool. The mixture was separated  
85 (using filter paper), the resulting solid sample has the potential of being processed further to  
86 obtain chitosan however the extract from deprotenization process contains some percentage  
87 of radical protein that will become a waste if not harnessed. The liquid extract was allowed to  
88 settle for 30mins. The concentrated slurry settled at the bottom of the beaker was collected  
89 (chito-protein), dried and stored for use.

90



91  
92 Fig. 1 : Fish scale



93  
94 Fig. 2: Fish scale flour

95

### 94 **2.3 Coagulation-Flocculation Experiment (Jar Test)**

95 The coagulation-flocculation experiments were performed using jar test apparatus. The  
96 operating variables investigated were; initial effluent pH, chito-protein dosage, settling time  
97 and operating temperature. The pH was controlled by adding either 1M HCl (acid) or 1M

98 NaOH (base). The VOW sample was mixed homogeneously before being fractionated into  
 99 beakers containing 250ml of suspension each. The desired amount of chito-protein was added  
 100 to each beaker containing the wastewater. Thereafter, the beakers were agitated at 250 rpm  
 101 (fast mixing) for 2 minutes and 30 rpm (slow mixing) for 20 minutes. The effect of pH was  
 102 studied at pH range (2 - 10) at varying chito-protein dosages in the range (0.5g – 2.5g) at  
 103 different settling time and constant temperature. Thereafter, the effect of settling time was  
 104 studied in the range (5 - 60 minutes) at varying coagulant dosages, optimum pH and constant  
 105 temperature. The effect of temperature was then studied in the range (30 – 60°C) at varying  
 106 settling time, optimum pH and coagulant dosage. The coagulation efficiency of the  
 107 coagulants was investigated in terms of turbidity removal. Prior to the test, the sample was  
 108 measured for turbidity, representing an initial turbidity. After settling at a specified time,  
 109 samples were collected at 2 cm depth beneath the surface of the water for further turbidity  
 110 measurement, representing the final turbidity. The residual turbidity (final turbidity) was  
 111 converted to TDSP (mg/L), using a calibration curve at intervals of 5mins. The efficiency of  
 112 turbidity removal was then evaluated using equation 1.

$$113 \quad \% \text{Removal} = \frac{T_0 - T}{T_0} \times 100 \quad (1)$$

114 Where;  $T_0$  is the turbidity of raw effluent and  $T$ , the turbidity of effluent after treatment.

#### 115 **2.4 Coagulation kinetic model description and theoretical principles**

116 The non-adsorptive kinetics of the process was modelled according to the description  
 117 reported by (Menkiti et al., 2015; Ugonabo et al., 2012).

118 For a system operating at equilibrium phase with negligible impact of external Equations 2  
 119 and 3 hold (Ugonabo et al., 2012):

$$120 \quad \mu_i = \bar{G}_i = \left[ \frac{\partial G}{\partial n_i} \right]_{P,T,n} = \text{a constant}$$

121 (2)

$$122 \quad D' = K_B \frac{T}{B}$$

123 (3)

124 Where:  $D'$  is diffusion coefficient;  $B$  is friction factor;  $K_B$  is Boltzmann's constant;  $T$  is  
 125 temperature;  $G$  is the total Gibbs free energy;  $n_i$  is the number of moles of component  $i$ ;  $\mu_i$  is  
 126 the chemical potential

127 for a case of mono dispersed, no break up and bi particle collision, floc formation depends  
 128 on the rate of successful particles collision. For a particular floc size ( $Z$ ) to be formed from  
 129 particles of sizes  $i$  and  $j$ , this rate can be expressed as (Ani et al., 2011; Ugonabo et al., 2012):

$$130 \quad \frac{dn_z}{dt} = \frac{1}{2} \sum_{i+j=z} \beta_{BR}(i, j) n_i n_j - \sum_{i=1}^{\infty} \beta_{BR}(i, k) n_i n_z$$

131 (4)

132 Where  $\beta_{BR}(i, j)$  is Brownian collision factor for flocculation transport mechanism.

133  $n_i n_j$  is particle aggregation concentrations for particles of size  $i$  and  $j$ , respectively.

134 According to Ugonabo et al (2012):

$$135 \quad \beta_{BR} = \frac{8}{3} \varepsilon_p \frac{K_B T}{\eta}$$

136 (5)

137 And  $K_R = 8\pi a D'$

138 (6)

139 Where:  $K_R$  is the Von smoluchowski rate constant for fast coagulation;  $a$  is particle radius;  
 140  $\varepsilon_p$  is the collision efficiency;  $\eta$  is the viscosity of the fluid medium.

141 Simplifying equations (6):

$$142 \quad K_R = \frac{4}{3} \frac{K_B T}{\eta}$$

143 (7)

144 Equations 4-5 could also be transformed to Eq. (7):

$$145 \quad K_m = \frac{1}{2} \beta_{BR}$$

146 (8)

147 Where:  $K_m$  is defined as Menkonu coagulation-flocculation rate constant accounting for  
148 Brownian coagulation-flocculation transport of destabilized particles at  $\alpha^{\text{th}}$  order.

149 For Brownian coag-flocculation (Ugonabo et al, 2012):

$$150 \quad -\frac{dN_t}{dt} = K_m N_t^\alpha$$

151 (9)

152  $N_t$  is the concentration of TDSP at time,  $t$

153 Practically, it has been observed that:  $1 \leq \alpha \leq 2$  (Ugonabo et al., 2012). Graphical  
154 representation of linear version of Eq. 9 at  $\alpha = 1$  or 2 should produce a linear graph from  
155 which  $K_m$  could be determined from the slope of either Equation 10 or 11:

$$156 \quad \alpha = 1: \quad \ln\left(\frac{1}{N}\right) = K_m t - \ln N_0$$

157 (10)

$$158 \quad \text{For } \alpha = 2: \quad \frac{1}{N} = K_m t + \frac{1}{N_0}$$

159 (11)

160 Where  $N_0$  is the initial  $N_t$  at time = 0

161  $N$  is  $N_t$  at upper time limit  $> 0$

162 Eq. (11) could be solved to obtain coagulation-flocculation period  $\tau_{1/2}$

$$163 \quad \tau_{1/2} = \frac{1}{(0.5N_0K_m)}$$

164 (12)

165 For Brownian controlled aggregation at  $t \leq 30$  min, Eq. (12) could be solved exactly to  
166 generate Eq.13

$$\frac{N_{m(t)}}{N_0} = \frac{\left[ \frac{t}{\tau_{1/2}} \right]^{m-1}}{\left[ 1 + \frac{t}{\tau_{1/2}} \right]^{m+1}}$$

167  
168 (13)

169 **2.5 Particle Variations Behaviour as a Function of Time.**

170 The particle variations behavior plots of turbidity removal from vegetable oil refinery  
171 wastewater (VOW) was investigated.

172

173 **2.6 Adsorption kinetic model description**

174 The influence of adsorption on the coagulation process was investigated. The jar test data were  
175 subjected to series of adsorptive analysis. Three kinetic models were studied which includes: Pseudo  
176 first order, Pseudo second order and Elovich kinetic model. Table 1 presents the linear and  
177 corresponding non-linear model equations.

178 **Table 1: Linear and non-linear kinetic models**

179	Kinetic equations	linear form	Non-linear	plot made	Eqn. No
180	Reference				
181	Pseudo-first-order (Okoye et al., 2013)	$\log(q_e - q_t) = \log q_e - \left(\frac{K_1 t}{2.303}\right)$	$q_t = q_e [1 - \exp(-k_1 t)]$	$\log(q_e - q_t)$ vs. t	(14)
183	Pseudo-second-order (15) (Okoye et al., 2013)	$t/q_t = \frac{1}{K_2 q_e^2} + \frac{t}{q_e}$	$q_t = \frac{k_2 q_e^2 t}{1 + k_2 q_e t}$	$\frac{t}{q_t}$ vs. t	
185	Elovich (Okoye et al., 2013)	$q_t = \left(\frac{1}{\beta}\right) \ln(\alpha\beta) + \left(\frac{1}{\beta}\right) \ln t$	$q_t = \left(\frac{1}{\beta}\right) \ln(1 + \alpha_1 \beta t)$	$q_t$ vs. t	(16)

188 *Where  $q_t$  and  $q_e$  = quantity adsorbed at a time and equilibrium respectively,  $K_1$  = pseudo*  
189 *first order constant,  $t$  = time,  $K_2$  = pseudo second order constant,  $\alpha\beta$  = Elovich constant*

190 **3.0 RESULTS AND DISCUSSION**

191 **3.1 Characterization of vegetable oil refinery wastewater (VOW) before and after**  
192 **coagulation**

193 The characterization result of the vegetable oil refinery wastewater before and after  
 194 coagulation process is presented in Table 2. The vegetable oil refinery wastewater possessed  
 195 high values of total suspended solids (TSS), biochemical oxygen demand (BOD), chemical  
 196 oxygen demand (COD), total suspended solids (TSS) and colour before treatment compared  
 197 with the national regulatory standard for effluent discharge. Table 2 shows that the values of TSS,  
 198 COD BOD among others recorded for the raw sample were well above national discharge standard,  
 199 hence there is need for treatment before discharge. These values were reduced drastically after the  
 200 coagulation treatment (see [table 2](#)), affirming the effectiveness of the coagulation in  
 201 achieving organic load reduction (Obiora-Okafo and Onukwuli, 2013).

202 Table 2: Characterization result of VOW before and after coagulation using FSC

Parameter	Before Coagulation	After Coagulation	WHO standard
Turbidity(NTU)	280	14	< 11.75
TSS (mg/l)	389.2	24	30.00
COD (mg/l)	933	65	NS
BOD (mg/l)	634	37	30
pH(-)	6.9	7.3	6.6-8.56
Colour (mg/l)	630.6	88	1
TS (mg/l)	688	58	500
TDS (mg/l)	298.8	34	50.00
Total hardness(mg/l)	43.8	19	500.00
Sulphate (mg/l)	18	2.4	1
Iron (mg/l)	0.632	0.13	0.3
Potassium (mg/l)	2.87	0.6	1
Magnesium (mg/l)	19.49	4.71	75
Lead (mg/l)	0.10	-	0.1

203

204 Note: NTU-nephelometric turbidity unit, TDS-total dissolved solids, TSS-total suspended  
 205 solids, COD-chemical oxygen demand and BOD -biochemical oxygen demand

206 **3.2 Characterization result**



### 207 3.2.1 Physiochemical characterization

208 The bio-coagulant extracted from the fish scale flour was subjected to proximate analysis. The  
209 properties measured are percentage moisture, crude protein, ash content, crude fibre,  
210 carbohydrates and lipid content. The characteristics of FSC presented in Table 3 show that it  
211 has a reasonably high content of protein (19.11%). This is an indication of its likely good  
212 performance as a coagulant for wastewater treatment.

213 **Table 3: Proximate analysis of FSC**

---

Moisture (%)	7.48
Crude protein (%)	19.11
Ash content (%)	25.08
Crude fibre (%)	3.05
Lipid content (%)	2.98
Carbohydrates (%)	42.3

---

214

### 215 3.2.2 FTIR analysis

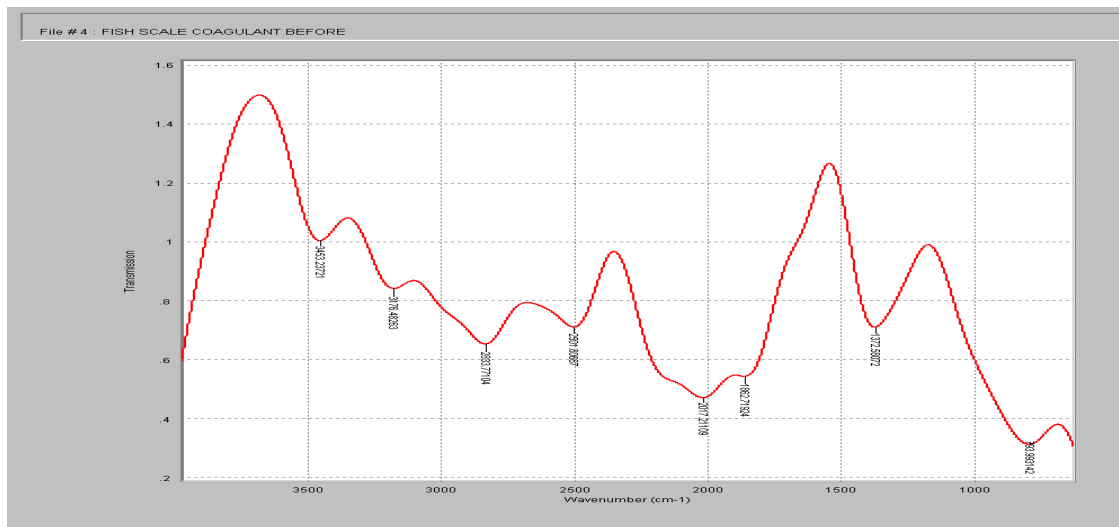
216

217 The FTIR spectra of the raw and extracted polymer (chito-protein) derived from fish scale are  
218 shown in figures 3 and 4 respectively. The results were analyzed based on the standard peaks  
219 as presented by Silverstein et al. (1981) for various functional groups. The comparison of the  
220 spectra results of the coagulant precursors and the synthesized coagulants indicates an  
221 obvious shift, disappearance and detection of new wave numbers. This observation could  
222 have existed as a direct consequence of the chemical reaction process involved in the  
223 coagulant synthesis and further elucidates the existence of improved/modified chemical  
224 species on the coagulants. This chemical modification could ultimately result in an improved  
225 coagulation performance by the respective coagulants. Table 4 provides detailed information  
226 on raw and extracted coagulant with respect to the various peaks that shifted, vanished or  
227 appeared. The wave number shifts in the spectra image of the coagulant are observed to range  
228 between  $\pm 2\text{cm}^{-1}$  to as high as  $\pm 147\text{ cm}^{-1}$  (see Table 4). Another important observation made  
229 with respect to Table 4 is that there were negligible wave number differences between FSF  
230 and FSC when compared to the other materials. This finding suggests a limited reactivity of  
231 the respective functional groups in FSF during the synthesis of FSC.

232 Vibrational peaks observed from the analysis are presented in table 4 and figures 3 and 4.

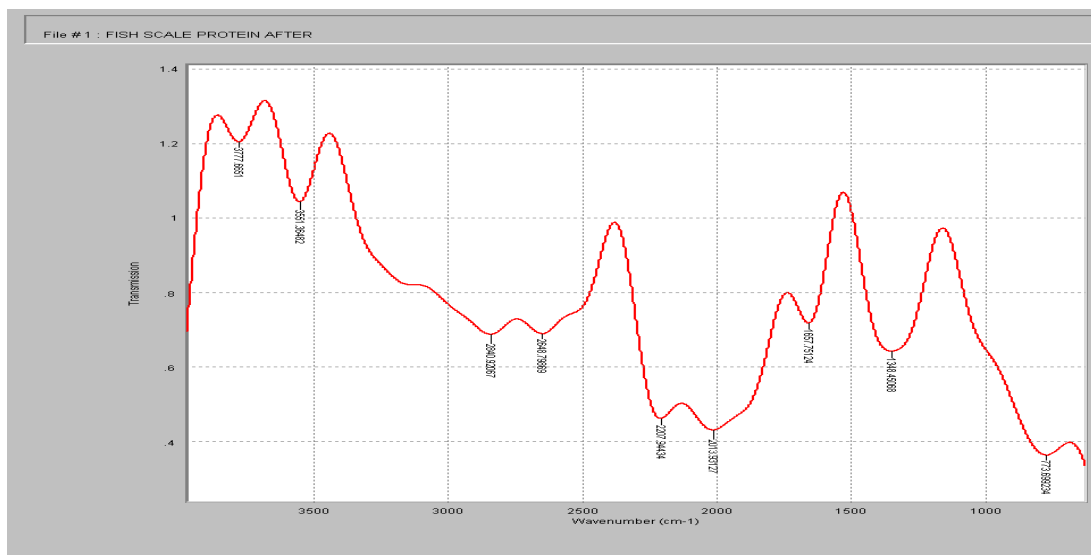
233 Usually the absorption peaks observed below  $500\text{ cm}^{-1}$  are not applicable for the

234 characterization of fish scale (Fernandez-Kim, 2004). At the higher wave number end of the  
 235 spectra, the C – H stretching region provides important information about the coagulants’  
 236 chemical composition. The distinct stretching band at wave numbers greater than 3000 cm<sup>-1</sup>  
 237 suggests the existence of aromatic ring groups in the coagulant structure (Günter and David,  
 238 2014). The peak at 793.9931cm<sup>-1</sup> can be attributed C-H bending vibration while that at  
 239 1348.451cm<sup>-1</sup> can be assigned to SO<sub>2</sub> asymmetric band. Additionally, the absorption peak at  
 240 3453.237cm<sup>-1</sup> which is within the range of 3200 and 3500 cm<sup>-1</sup> which were characteristic of  
 241 N-H stretching of amides (Stuart, 2004).



242

243 Figure 3: FTIR spectrum analysis of FSF sample



244

245 Figure 4: FTIR spectrum analysis of FSC sample

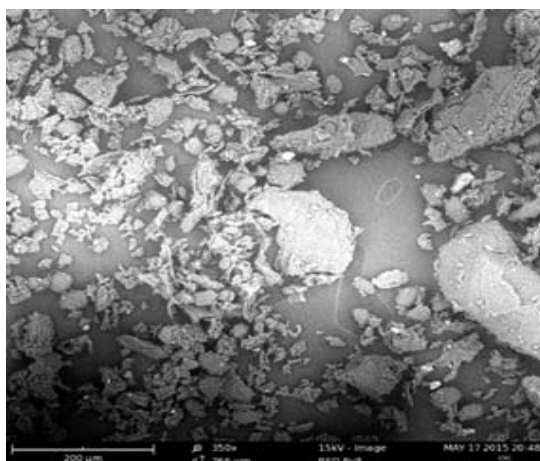
246 Table 4: FTIR table for vibrational peaks of fish scale (FSF and FSC)

Peak ( $\text{cm}^{-1}$ )			
FSF	FSC	Differences	Assignment
793.9931	773.6992	20.29	Out – of – plane C – H bending
1372.581	1348.451	24.13	SO <sub>2</sub> asymmetric band
x	1657.751	x	NO <sub>2</sub> asymmetric stretching
1862.719	x		C = O stretching
2017.211	2013.944	3.28	Metal carbonyl C = O
x	2207.94	x	
2501.807	2648.799	146.99	Phosphoric acid and Ester O – H
2833.771	2840.921	7.15	C – H stretching of aldehyde
3176.483	x	x	O – H stretching of carboxylic acid
3453.237	x	x	N – H stretching
x	3551.365	x	Si – OH stretching

247

### 248 3.2.3 Scanning electron microscopy (SEM) characterization of FSC and FSC

249 The SEM technique, a powerful tool for analysing the surface morphological make-up of the  
 250 polymeric coagulants was employed. SEM image was used to elucidate the surface texture  
 251 and morphology of the synthesized coagulant. The result of the SEM studies for the raw (fish  
 252 scale flour) extracted (FBC) samples were presented in plates 1 and 2.



253

254 Plate 1: SEM micrograph of FSF

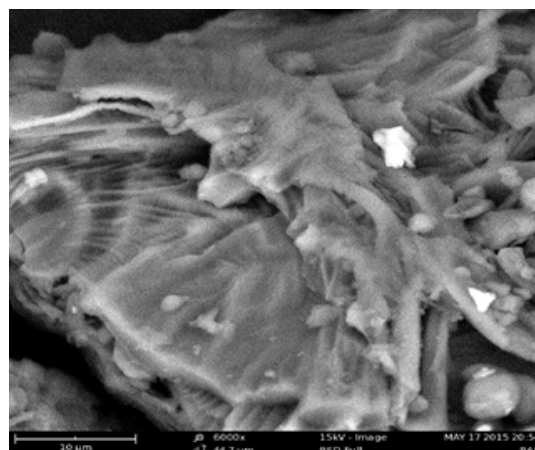


Plate 2: SEM Micrograph of FSC

255 Plates 1 and 2, show the SEM micrographs of fish scale flour and fish scale chito-protein  
256 respectively. Plate1 was mainly characterized by smooth surface with seemingly compact  
257 structures. It also exhibits the appearance of tiny homogenous pores. While, Plate 2 shows the  
258 existence of irregular granular structure on the coagulant morphology. The appearance of  
259 irregular platelets on plate 2 shows that fish scale coagulant (FSC) has rough edges which  
260 may be attributed to high brittle property of the coagulant, (Obiora-Okafo et al., 2014). Also,  
261 according to Obiora-Okafo (2011), irregular granular structures are desirable characteristics  
262 of any coagulant with regards to adsorbing and bridging of colloidal particles and further  
263 enhancing the sedimentation of flocs. Multiple pores can also be visualized on plate 2; these  
264 pores are available sites for particles adsorption.

### 265 **3.5 Factor Sensitivity studies**

266  
267 Various factors influence the coagulation performance of any given coagulant. The influences  
268 of the variation of some of these factors are highlighted in section 3.5.1 to 3.5.3;

269

#### 270 **3.5.1 Effect of FSC dosages and setting time on TDSP removal efficiency**

271

272 The effect of coagulant dosage (FSC) at different settling time on TDSP removal efficiency  
273 from vegetable oil refinery wastewater was analysed at initial pH of the wastewater. Fig. 5  
274 shows the plots of removal efficiency of TDSP against settling time at varying dosages. The  
275 result of the turbidity removal with respect to FSC dose is presented in Fig. 5. The dosage  
276 studied varied from 0.5-2.5g of FSC in 500ml of VOW. The graph (Fig.5) indicates that the  
277 removal TDSP increased with increase in the coagulant dosage. The percentage turbidity  
278 removal recorded for coagulant dose of 1g was 74.7% at 30min. Similarly, at a coagulant  
279 dose of 1.5g over the same time, the percentage TDSP removal was 84.0%. The increase in  
280 the TDSP removal with an increase in FSC dose could be attributed to the availability of  
281 large content of protein created by more quantity of coagulant deposited to the wastewater  
282 which aid to fast coagulation process.

283

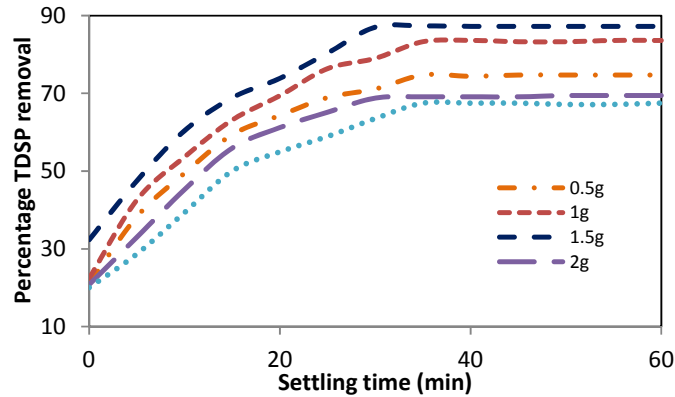


Fig 5: Effect of coagulant dosage

### 3.5.2 Effect of pH on turbidity removal efficiency

The effect of pH was studied at the varying coagulant dosage, temperature of 30°C, and time of 60min as shown in Fig.6. The pH of the wastewater was varied from 2-10 using H<sub>2</sub>SO<sub>4</sub> and NaOH. The result is shown in Fig. 6 for TDSP. An optimum TDSP removal efficiency of 84% was obtained at pH of 2 with 1.5g optimum coagulant dose. This shows that the treatment process performs better when the solution is in acidic medium. In addition, after the pH of 2, the removal efficiency of the particles decreased continuously till the minimum value was attained, this trend can be attributed to decrease in solubility of coagulant with increase in pH. Hence, it was evident that FSC may not be very effective in alkaline solution. Similar works were reported by Devi et al (2012).

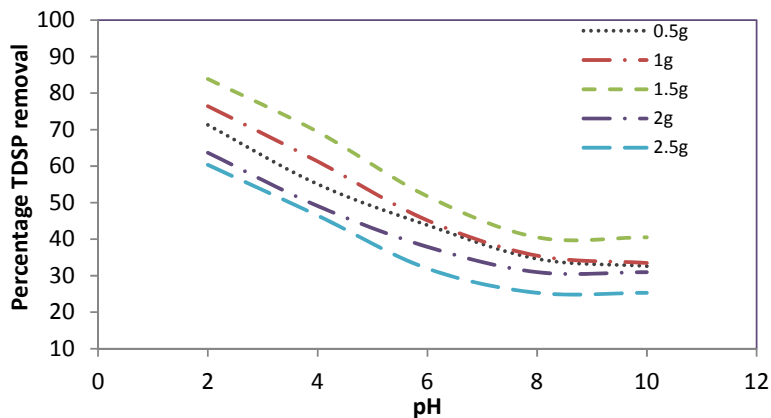
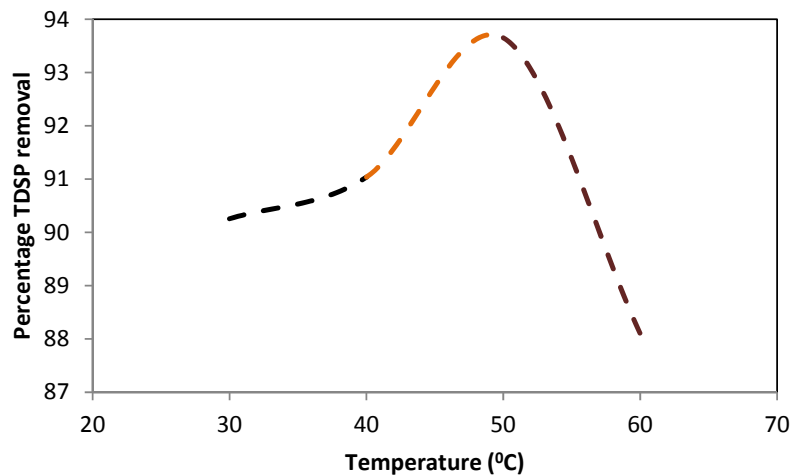


Fig 6: Effect of pH

### 3.5.3 Effect of temperature on TDSP removal efficiency

304  
305 The effect of temperature on the coagulation efficiency was investigated at the best pH and  
306 best coagulant dose while varying the temperature between 30 – 60°C. From the efficiency  
307 analysis, it was observed that the coagulation efficiency varies directly with temperature to  
308 the maximum (Fig. 7) and decreased thereafter. The ascending part can be attributed to  
309 particle excitement; hence at this stage more flocs are formed. After the maximum stage  
310 (50°C), decrease in particle removal with temperature was observed at temperature of 60°C  
311 This could be as a result of denaturation of the coagulant particles which may cause slight  
312 inhibition of the process. Similar result was obtained by Babayemi et al. (2013)  
313



314

315 **Fig. 7: Effect of temperature on turbidity (%) removal**

### 316 **3.6 Coagulation Kinetics**

317 The kinetics of TDSP removal was evaluated to study the effect of time on the particle  
318 movement from the bulk of the effluent sample to the surface of the coagulant after charge  
319 neutralization and destabilization, the kinetic plot ( $\frac{1}{C_t}$  vs  $t$ ) that described the rate of particle  
320 transport is presented in Fig. 8, while the calculated parameters are presented in table 5.

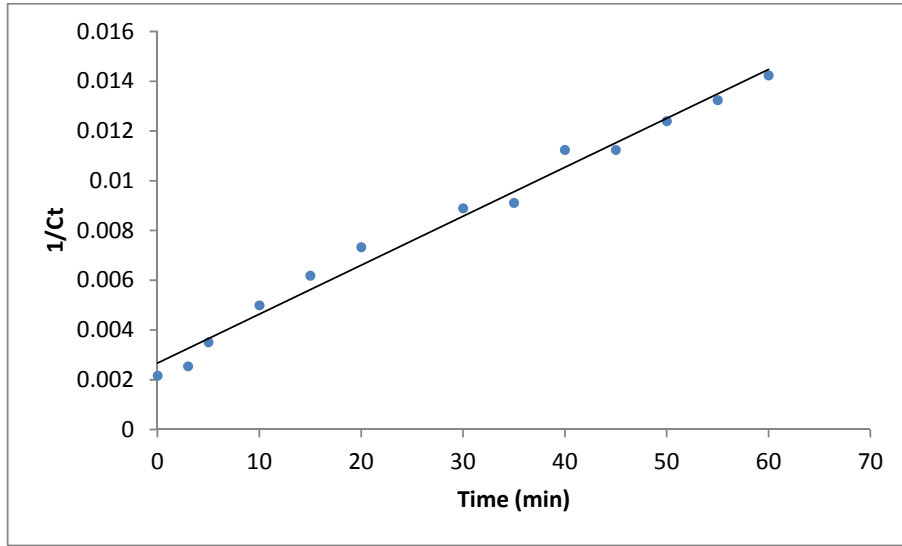


Fig. 8: Plot of 1/Ct against settling time for

321

322

323

324

325 Brownian transport of destabilized particles ( $K_m$ ) for the rate constant was evaluated from the

326 slope of the kinetic plot of 1/Ct against t (Fig 8), while the Von smolushoski's coagulation

327 constant ( $K_R$ ) accounts for the rate of rapid coagulation was determined based on equation

328 11. For perikinetic coagulation with a constant order of 2, the difference between  $K_m$  and  $K_R$

329 accounts for the rate of particle flocculation ( $K_f$ ). The  $K_m$  was obtained as 2E-05g/min while

330  $K_m$  was obtained as 4.86E-21. The rate of particle flocculation was 0.00002g/min. The number

331 of effective collision was estimated as a function of particle collision efficiency ( $\epsilon_p$ ). Higher

332 value of ( $\epsilon_p$ ) obtained in the system suggests that more collision leads to floc formation.

333 Table 5 shows the parameters obtained. From table 5, it can be observed that  $K_m \gg K_R$

334 which shows that  $K_R$  is quite negligible relative to  $K_m$ . The result suggests that the entire

335 process is greatly influenced by the rate of floc formation than the actual rate of coagulation.

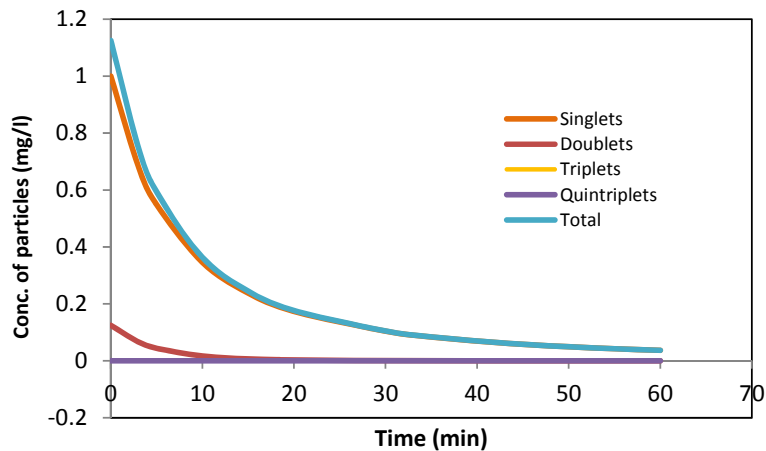
**Table 5: coagulation kinetic parameters**

Parameters	
$K_m$ (g.min)	2.00E-05
$R^2$	0.9245
$\beta Br$ (g.min)	0.00004
$\tau_{1/2}$ (min)	50.00
R	1.11E-05

$\epsilon_p$	4.12E+15
$K_R$	4.86E-21
$D'$	1.74E-17
B	0.000239917
A	2.0000

336 **3.7 Particle distribution**

337 The total number of turbidity concentration,  $N_t$  and the concentration of the species  $N_i$  both  
338 decrease monotonically with increasing time. From the plot (Fig. 9), the concentrations of  $N_2$   
339 ( $t$ ),  $N_3$  ( $t$ ) and  $N_4$  ( $t$ ) pass through a maximum (Santhanam et al., 2014). This is because they  
340 are not present at  $t = 0$  and  $N_0 = 0$ . The number of singlet ( $N_1$ ) can be seen to decrease more  
341 rapidly than the total number of particles  $N_i$ . This happens as a result of increasing number of  
342 particles concentration on aggregate formation with time (Menkiti and Ejimofor, 2016). Here,  
343 the total number of particles decreases according to a bimolecular reaction. From the plot, it  
344 can be observe that the lower the value of  $K$ , the higher the coagulation time  $T_{ag}$  with respect  
345 to its  $N_0$  and the more the effect of high period of particle distribution (Obiora et al. 2014).  
346 At low  $K$  the rate process is very slow which gives rise to more time for the coagulation-  
347 flocculation process. Fig. 9 shows the effect of high period of particle distribution. Here, the  
348 decrease of singlets from initial particle concentration and increase in doublets, triplets and  
349 quadruplets from zero concentration occur. The sum of all the distribution particles from  
350 singlets ( $N_1$ ), doublets ( $N_2$ ), triplets ( $N_3$ ) and quadruplets ( $N_4$ ) display the overall effects of  
351 high period on the reactor. This suggests low rate of particle aggregation and poor particle  
352 removal efficiency (Menkiti and Ejimofor, 2016).



353

354 Fig.9: Particle distribution plot for TDSP removal

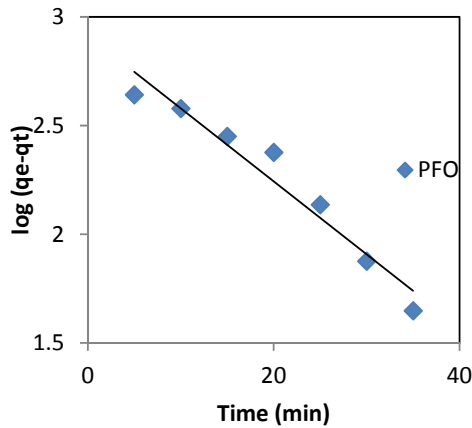
355

356

**3.6 Coag-adsorptive kinetic studies**

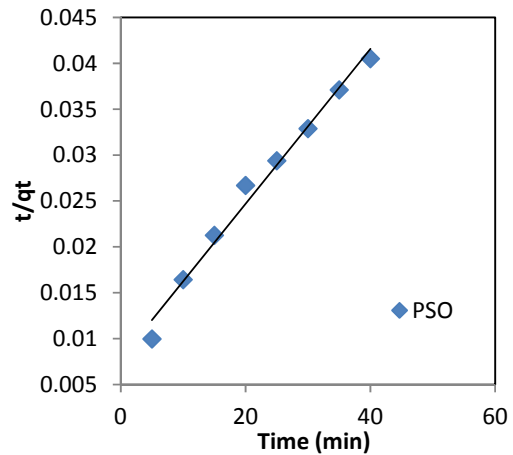


357 Coagulation is known to be a multi-component process where four mechanisms can be  
358 identified. The mechanisms include; double layer compression, adsorption and charge  
359 neutralization, sweep flocculation and adsorption and inter-particle bridging. These  
360 mechanisms are grouped into adsorptive and non-adsorptive components. To describe the  
361 adsorptive component of the process, adsorption kinetic models were used to model the  
362 coagulation kinetic data obtained during the experimental studies. For this present studies,  
363 three (3) kinetic models were considered which includes: PFO, PSO and Elovich kinetic  
364 models. Figs. 10, 11 and 12 show the linear plots of PFO, PSO and Elovich kinetic models.  
365 While Fig. 13 shows the comparative relationship between the nonlinear model data and the  
366 experimental data. Also, table 6 shows the calculated model parameters, their statistical T-  
367 Test, F-test, STD and Chi test estimated can also be identified in the same table 6.



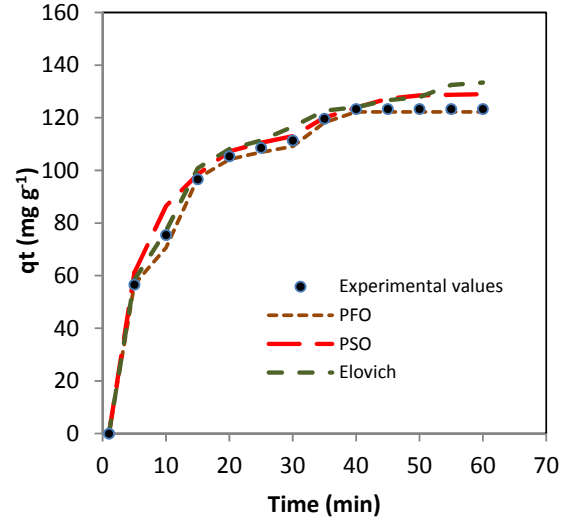
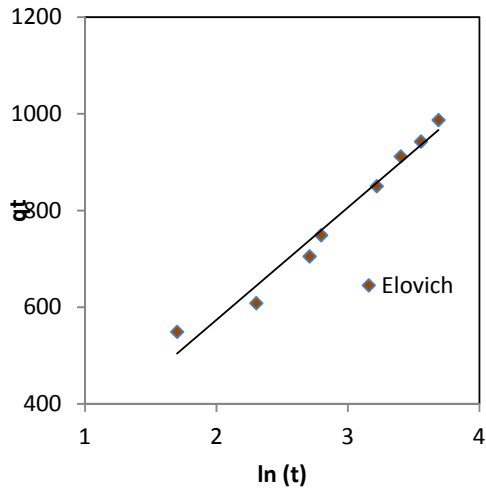
368

Fig. 10: Linear plot of PFO kinetic model



369

Fig. 11: Linear plot of PSO kinetic model



370  
371 Fig. 12: Linear plot of Elovich kinetic  
372 kinetics

Fig. 13 Non-linear kinetic modeling of the coag-adsorptive

**Table 6: kinetic parameters for linear and non-linear kinetic models**

PSO		PFO		Elovich	
K (linear)	0.000846	K (linear)	0.01624	$\beta$ (linear)	0.046268
$R^2$ (linear)	0.9974	$R^2$ (linear)	0.9873	$\alpha$ (linear)	24.89146
K(non-linear)	0.00283	K (non-linear)	0.01624	$R^2$ (linear)	0.9607
$q_e$ (linear)	129.9479	$q_e$ (linear)	107.9941	$\beta$ (non-linear)	0.163284
$q_e$ (non-linear)	129.7413	$q_e$ (non-linear)	109.0498	$\alpha$ (non-linear)	44.72479
$R^2$ non-linear	0.9945	$R^2$ non-linear	0.9909	$R^2$ (non-linear)	0.9738
T-test	0.036036	T-test	0.000715	T-test	0.000232
F-test	0.712126	F-test	0.886854	F-test	0.835209
Chi test	0.99906	Chi test	0.994527	Chi test	0.996882
STD	20.08663	STD	20.8065	STD	21.98474
$\Delta q_e$	0.206587	$\Delta q_e$	1.0557	$\Delta q_e$	10.05778

373 The Pseudo first order and pseudo second order models assume that the adsorptive  
374 component of coagulation is a pseudo chemicals reaction, while the kinetic data follow  
375 Elovich model if the adsorption is chemical in nature. In this present study, it was observed  
376 that the coefficient of correlation for models considered were above 0.9 for both linear and  
377 non-linear studies. Hence the difference between  $q_{(e \text{ exp})}$  and  $q_{(e \text{ cal})}$  ( $\Delta q_e$ ) was used as the  
378 basis of model comparison. Where  $q_{(e \text{ exp})}$  is the quantity adsorbed at equilibrium time, while  
379  $q_{(e \text{ cal})}$  is model generated data. From table 6, the models with  $(\Delta q_e) \geq 2$  were considered as  
380 having poor description of the experimental kinetic data. Hence, pseudo second order and  
381 pseudo first order kinetic models with  $(\Delta q_e) < 2$  were considered.

#### 382 4.0 CONCLUSION

383 Fish scale has been identified as a potential source of coagulation agent for the removal of  
384 turbidity from vegetable oil industry effluent. Some of the parameters that control bio-  
385 coagulation were found to include coagulation pH, coagulant dosage, and coagulation  
386 temperature. It was observed that the percentage turbidity removal increased with increase of  
387 the settling time. The optimum contact time, pH and temperature were 30 min, 2 and 323K  
388 respectively. By applying 3 different linear and nonlinear kinetic models to evaluate the  
389 optimum parameter sets; Pseudo first order and Pseudo second order models were found to be  
390 the best two most suited models (judging by the maximum correlation coefficient,  $R^2$  and  
391 least  $\Delta q_e$  value. Using statistical tools (F-test and student's t-test) the predicted kinetic data  
392 were adjured statistically significant. The FT-IR spectrum confirmed the chemical structures  
393 of both the fish scale flour and their corresponding coagulant (FSC) with the functional ester  
394 groups present. The kinetics of the coagulation/flocculation reaction presented showed that  
395 the reaction followed second order kinetic model. Since, fish scale performed very well in the  
396 coagulation studies performed, there is therefore great possibility of replacing chemical  
397 coagulants with less hazardous and efficient bio-coagulants.

398

#### 399 **ABBREVIATIONS**

400 VOW: Vegetable oil refinery wastewater  
401 FSF: Fish scale flour  
402 FSC: Fish scale coagulant  
403 TDSP: Total suspended and dissolved particles  
404 FTIR: Fourier transforms infrared  
405  $T_o$ : Turbidity of raw effluent  
406 T: Turbidity of effluent after treatment  
407 TSS: Total suspended solid  
408 TS: Total solid  
409 COD: Chemical oxygen demand  
410 BOD: Biochemical oxygen demand

411

#### 412 **REFERENCES**

413

414 Ani J.U, Menkiti,M.C and Onukwuli,O.D (2010). Coagulation and Flocculation behaviour of  
415 snail shell coagulant in fibre-cement plant effluent, J.Eng.Appl.Sci.67, 2.

- 416 APHA (1998). Standard Methods for Water and Waste Water Examination. 16<sup>th</sup> Edition,  
417 American Public Health Association (APHA), Washington DC, USA
- 418 Babayemi K.A., Onukwuli O.D & Okewale A.O. (2013). Coag-Flocculation of Phosphorus  
419 Containing Waste Water Using Afzella-Africana Biomass. *International Journal of*  
420 *Applied Science and Technology* Vol. 3 No. 6, pp 43-50.
- 421 Devi G., Shinoon A.H. and Sekhar G.C., (2012). Treatment of vegetable oil mill effluent  
422 using crab shell chitosan as adsorbent. *International journal of Environmental*  
423 *Science and Technology* 9(4) DOI:10.1007/s13762-012-0100-4
- 424 Divakaran R. and Pillai V.N.S. (2001). Flocculation of kaolinite suspension in water by  
425 chitosan, *Water Res.* 35, 3904-3908.
- 426 Dkhissi O., El Hakmaoui A., Souabi S., Chatoui M., Jada A., Akssira, M. (2018). Treatment  
427 of vegetable oil refinery wastewater by coagulation-flocculation process using the  
428 cactus as a bio-flocculant. *Journal of Materials and Environmental Sciences*, 9 (1),  
429 18-25.
- 430 Fernandez-Kim S. (2004), Physiochemical and Functional properties of crawfish chitosan as  
431 affected by different processing protocols, M.Sc Thesis, Louisiana State University  
432 and Agricultural and Mechanical College, USA.
- 433 Günter, G and David S.M (2014) Handbook of spectroscopy, 2nd edn. John Wiley & Sons,  
434 Hoboken. <https://doi.org/10.1002/9783527654703>.
- 435 Menkiti M.C, Ganesan S, Ugonabo V. I, ' Menkiti N. U, Onukwuli O.D., (2015), Factorial  
436 optimization and kinetic studies of coagulation-flocculation of brewery effluent by  
437 crab shell coagulant; *Journal of the Chinese Advanced Materials Society*.
- 438 Menkiti, M. C., Ejimofor, M. I., (2016). Turbidimetric Approach on the study of Adsorptive  
439 component of paint effluent coagulation using snail shell extract, *Arabian journal for*  
440 *science and Engineering* 41,7, 2527-2543.
- 441 Moka, K.B (2015). Technical Report on SIWES undertaken at a vegetable oil Industry.  
442 Nnamdi Azikiwe University, Nigeria.

- 443 Obiora-Okafo, I. (2011). Treatment of brewery wastewater using coagulation-flocculation  
444 and adsorption techniques. Unpublished Masters' Thesis, Department of Chemical  
445 Engineering, Nnamdi Azikiwe University Awka, Nigeria. 65.
- 446 Obiora-Okafo, I.A., and Onukwuli, O.D. (2013). Utilization of sawdust (*Gossweilerodendron*  
447 *balsamiferum*) as an adsorbent for the removal of total dissolved solid particles from  
448 wastewater. *International Journal of Multidisciplinary Sciences and Engineering*,  
449 4(4): 45 – 53.
- 450 Obiora-Okafo, I.A., Menkiti, M.C., and Onukwuli, O.D. (2014). Utilization of response  
451 surface methodology and factor design in micro organic particles removal from  
452 brewery wastewater by coagulation / flocculation technique. *Inter. J. of Appl. Sci.*  
453 *and Maths.*, 1(1): 15 – 21.
- 454 Okey-Onyesolu, C.F. Onukwuli, O. D. Okoye, C. C. and Nwokedi I. C. (2016). Removal of  
455 heavy metal pb(II) ions from aqueous solution using pentaclethra macrophylla and  
456 tetracarpidium conophorum seed shells based activated carbons: equilibrium,  
457 kinetics and thermodynamics studies. *British Journal of Applied science &*  
458 *Technology*, 16(6): 1-20.
- 459 Okoye, C. C, Onukwuli, O. D, Okey-Onyesolu, C. F and Nwokedi, I. C (2013): Adsorptive  
460 Removal of Erythrosin B Dye onto *Terminalia Catappa* Endocarp Prepared  
461 Activated Carbon: Kinetics, Isotherm and Thermodynamics Studies.
- 462 Oladoja N.A. and Aliu Y.D. (2008); Evaluation of plantain peelings ash extract as coagulant  
463 aid in the coagulation of colloidal particles in low pH aqua system, *Water Quality*  
464 *Research Journal*, Canada.
- 465 Ozacar, M. and Sengil, I.A. (2002). Effectiveness of tannins obtained from *velonia* as a  
466 coagulant aid for dewatering of sludge. *Water res.* 34(4); 1407-1412.
- 467 Roussy J., Chastellan P., Vooren M. and Guibal E. (2005). Treatment of ink-containing waste  
468 water by coagulation/flocculation using biopolymers, *Water SA* 31 (3), pp 369-376.
- 469 Santhanam Needhidasan, Melvin Samuel, and Ramalingam Chidambaram (2014). Electronic  
470 waste – an emerging threat to the environment of urban India. *J. Environ Health Sci*  
471 *Eng.* doi: 10.1186/2052-336X-12-36.

- 472 Silverstein, R.M.; Bassler, G.C.; and Morrill, T.C. (1981). Spectrometric Identification of  
473 Organic Compounds. 4th ed. New York: John Wiley and Sons. New York, USA.
- 474 Stuart, B (2004) Infrared spectroscopy: fundamentals and applications. John Wiley & Sons,  
475 Hoboken.
- 476 Ugonabo, V.I., Menkiti, M.C., Onukwuli, D.O. (2012). Effect of coag-flocculation kinetics  
477 on telfairia occidentalis seed coagulant (TOC) in pharmaceutical wastewater.  
478 International Journal of Multidisciplinary Sciences and Engineering, 3(9), 22-33.
- 479 Xu C.R., Yan Z.C. and Wang Y.C.(2009); Recycle of alum recovered from water treatment  
480 studies in chemically enhanced water treatment; Journal of hazardous materials 161  
481 pp 663-669.